



Contents lists available at SciVerse ScienceDirect

Spectrochimica Acta Part A: Molecular and Biomolecular Spectroscopy

journal homepage: www.elsevier.com/locate/saa

Fluorescent substituted amidines of benzantrone: Synthesis, spectroscopy and quantum chemical calculations

Svetlana Gonta^{a,*}, Maris Utinans^b, Georgii Kirilov^c, Sergey Belyakov^d, Irena Ivanova^c, Mendel Fleisher^d, Valerij Savenkov^a, Elena Kirilova^c

^aLaboratory of Microbial Storage Product Research, Institute of Microbiology and Biotechnology, University of Latvia, Kronvalda blvd. 4, Riga LV-1586, Latvia

^bFaculty of Materials Science and Applied Chemistry, Riga Technical University, Azenes str. 14, Riga LV-1048, Latvia

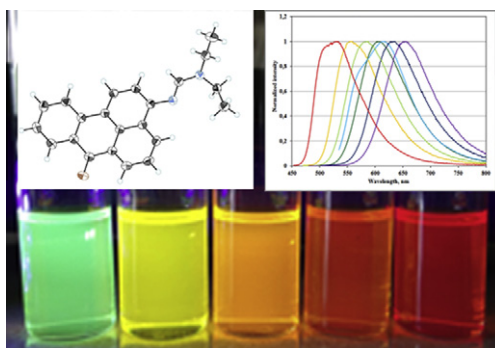
^cDepartment of Chemistry and Geography, Faculty of Natural Sciences and Mathematics, Daugavpils University, Vienibas str. 13, Daugavpils LV5401, Latvia

^dLatvian Institute of Organic Synthesis, Aizkraukles str. 21, Riga LV-1006, Latvia

HIGHLIGHTS

- ▶ A series of novel benzantrone dyes containing amidino group were synthesized and characterized.
- ▶ Spectroscopic properties of the new molecules were examined by FT-IR, NMR and UV techniques.
- ▶ Solvatochromic effect was studied. X-ray crystal structures were determined.
- ▶ HOMO and LUMO energies, molecular electrostatic potential distribution and dipole moments were calculated.

GRAPHICAL ABSTRACT



ARTICLE INFO

Article history:

Received 26 July 2012

Received in revised form 4 September 2012

Accepted 9 September 2012

Available online 12 October 2012

Keywords:

Benzantrone dyes
Fluorescence solvatochromism
Substituted amidines
Crystal structure
Solid-state luminescence

ABSTRACT

Several new substituted amidine derivatives of benzantrone were synthesized by a condensation reaction from 3-aminobenzo[de]anthracen-7-one and appropriate aromatic and aliphatic amides. The obtained derivatives have a bright yellow or orange fluorescence in organic solvents and in solid state. The novel benzantrone derivatives were characterized by TLC analysis, ¹H NMR, IR, MS, UV/vis, and fluorescence spectroscopy. The solvent effect on photophysical behaviors of these dyes was investigated, and the results showed that the Stoke's shift increased, whereas quantum yield decreased with the growth of the solvent polarity. The structure of some dyes was confirmed by the X-ray single crystal structure analysis. AM1, ZINDO/S and *ab initio* calculations using Gaussian software were carried out to estimate the electron system of structures. The calculations show planar configurations for the aromatic core of these compounds and two possible orientations of amidine substituents. The calculation results correlate well with red-shifted absorption and emission spectra of compounds.

© 2012 Elsevier B.V. All rights reserved.

Introduction

Design and synthesis of new fluorescent molecules is of continuing interest for understanding the fundamental electronic structure of molecules, as well as for many applications in research

and industry. Especially donor–acceptor π -conjugated organic materials have attracted considerable interest owing to their potentially wide application in the development of electro- and photoactive materials [1,2]. Such fluorescent dyes have a very wide range of applications in chemical and biological research.

Benzo[de]anthracen-7-one dyes in particular have found many applications because they provide a whole range of colours among which the most popular are red, orange, and yellow [2]. Many

* Corresponding author. Tel.: +371 67034889.

E-mail address: svetago7@gmail.com (S. Gonta).

benzanthrone derivatives are strongly fluorescent and that is why widely used as a laser dye [3], daylight fluorescent pigment [4], and lipophilic fluorescent probe for biochemical and medicinal investigations [5,6]. These probes are used to study microviscosity and fluidity of biological membranes because benzanthrone derivatives such as many fluorophores are characterized by fluorescence properties that are dependent on their environment.

For several years our research group has been working on benzanthrone dyes with D- π -A architecture, appeared to be particularly interesting because these dyes ultimately lead to prospective luminescent materials. In previous works, a series of benzanthrone amines and amidines were prepared [7–9]. These solvatochromic fluorescent substances have a large extinction coefficient and a significant Stokes shift. The obtained results testify that the fluorescence of synthesized amidino derivatives is sensitive to the change in polarity of surrounding, and fluorescence in the red region (above 600 nm) of spectrum contributes to a high analytical sensitivity of the method using these fluorophores [10].

Bearing this in mind, and in connection with our interest in synthesis, characterization, and application of a fluorescent probe, we have extended our preliminary investigations related to the fluorescent derivatisation of the benzanthrone core by including new substituents in the chromophoric system in order to find fluorescent dyes with prospective applications.

Compounds containing an amidine group have played important roles as ligands for various complexes of s-, p-, d- and f-block metals in organometallic chemistry [11]. It is known that substituted N-aryl amidines display an intense luminescence in solutions [9,10,12]. Moreover, the use of amidinate-ligated iridium complexes for fabrication of high efficiency phosphorescent organic light-emitting devices has been recently demonstrated [13]. Therefore it was of interest to prepare new luminescent dyes containing an electron-donating amidine group and an electron-accepting carbonyl group linked by an aromatic spacer. Herein, we present the facile synthesis and characterization of N-substituted amidino derivatives based on benzo[de]anthracen-7-one. The optical properties and crystal structure of novel synthesized compounds is studied in the present work. Quantum chemical calculations are also presented in order to demonstrate the electronic structures and properties of synthesized dyes.

Experimental

General

All reagents were of analytical grade (Aldrich Chemical Company) and were used as received. The progress of chemical reactions and purity of products were monitored by a thin-layer chromatography (TLC) on silica gel plates, Silufol UV254, 15 × 15, 0.2 mm, using the solvent system benzene/acetonitrile (3:1) as eluent. Column chromatography on silica gel was carried out on the Merck Kieselgel (230–240 mesh) with benzene as eluent. Melting points were measured on a Kofler apparatus and were not corrected. IR spectra were recorded on the SHIMADZU Prestige-21FT spectrometer in KBr pellets. ¹H NMR spectra were recorded on the Bruker AVANCE300 spectrometer operating at 300 and 75 MHz in DMSO-d₆ or CDCl₃ (with TMS as an internal standard) at an ambient temperature. The chromatomass spectroscopic studies were carried out using the Shimadzu QP2010 chromatograph with EI ionization, 70 eV, the mass range 39–400 *m/z*. The thermal gravimetric analyses (TG-DSC) were carried out with an Exstar6000 TG/DTA 6300 thermal analyzer with a heating rate of 10 K min⁻¹ in the temperature interval 30–400 °C. The quantum chemical calculations were performed using the AM1 [14,15], ZINDO/S [16–18] and *ab initio* (using DFT approach [19]) methods.

General procedure for the synthesis of substituted amidines

3-Aminobenzanthrone was prepared by nitration of benzanthrone and the following reduction of the obtained 3-nitro-derivative according to the literature procedure [20,21].

Procedure A (for amidines 3, 4, 8–10)

To the solution of 0.50 g (2.0 mmol) amine 1 in 2–3 ml of appropriate amides, the phosphorus oxychloride (0.2 ml, 2.1 mmol) was added dropwise under stirring. The resulting mixture was heated for 3 h at 90–100 °C. After cooling to the ambient temperature, the crude product that precipitated on pouring into 50 ml of 2% NaOH water solution was filtered, washed with water, and dried.

Procedure B (for amidines 2, 5, 6, 7)

To the solution of 0.50 g (2.0 mmol) amine and 2.5 mmol of appropriate amides in 5 ml toluene, the phosphorus oxychloride (0.2 ml, 2.1 mmol) was added dropwise under stirring. The resulting mixture was heated for 3 h at 90–100 °C. After cooling to the ambient temperature, toluene evaporated in vacuum and the mixture was neutralized by 50 ml of 2% NaOH water solution, the crude product was filtered, washed with water, and dried.

Spectroscopic measurements

Spectral properties of the investigated compounds were measured in chloroform and ethanol solutions with concentrations 10⁻⁵ M at an ambient temperature in 10 mm quartz cuvettes. All solvents were of p.a. or analytical grade. The absorption spectra were obtained using the UV-visible spectrophotometer “Specord’s UV/vis”. The fluorescence emission spectra were recorded on a FLS920 (Edinburgh Instruments Ltd.) spectrofluorimeter using Rhodamine 6G ($\Phi_0 = 0.88$) as a standard.

X-ray crystallography study

Diffraction data were collected on a Bruker-Nonius KappaCCD diffractometer using graphite monochromated Mo K α radiation ($\lambda = 0.71073$ Å). The crystal structures were solved by direct methods and refined by full-matrix least squares. For further details, see crystallographic data for these compounds deposited with the Cambridge Crystallographic Data Centre as Supplementary Publications. Copies of the data can be obtained, free of charge, on application to CCDC, 12 Union Road, Cambridge CB2 1EZ, UK.

Results and discussion

Synthesis and characterization

A number of different methods are available for the synthesis of substituted amidines. A traditional preparation method involves condensation of secondary amine and amide in presence of phosphorus oxychloride [22]. The target dyes were synthesized in high yields by condensation of 3-amino-benzanthrone (**1**) with

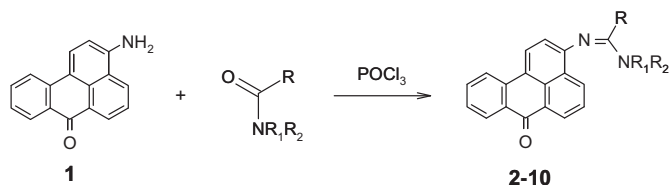


Fig. 1. Synthesis of benzanthrone amidines 2–10.

Table 1
Substituents, yields and identification data for prepared dyes **2–10**.

Compound	R	R ₁	R ₂	Yield (%)	M.p. (°C)	R _f (benzene: acetonitrile 3:1)
2	Me	H	Ph	52	244.2	0.68
3	H	H	Me	67	243.5	0.35
4	H	Et	Et	90	159.4	0.71
5	Me	H	4-MeC ₆ H ₄	82	250.0	0.57
6	H	H	Ph	65	247.1	0.66
7	H	Me	Ph	92	226.5	0.75
8	H	H	H	80	250.8	0.37
9	Me	H	Me	87	202.1	0.06
10	H	H	Et	85	218.2	0.36

appropriate amides using phosphorus oxychloride as a condensation agent. This synthetic route is outlined in Fig. 1.

In this paper, development of two synthetic procedures (A and B) is described. Method A was used for liquid amides, with its excess as reaction media. Method B was employed for solid amides, using toluene as a solvent for reacting compounds. Target products were readily obtained by recrystallization from chloroform or benzene in good yields (Table 1).

The obtained amidine derivatives are crystalline compounds colored from yellow to deep red. The reaction and purity of products were monitored by a thin-layer chromatography. IR, ¹H NMR, and mass spectroscopic studies confirmed the chemical structure of the new dyes **2–10**. The structures of prepared derivatives were determined by NMR spectroscopy, based on the analysis of H–H coupling constants and chemical shifts. In the ¹H NMR spectra of the dyes, the signals of appropriate alkyl group and multiplet signals (from δ 6.50 to 9.00 ppm) of aromatic protons of benzanthrone ring were found (see Supplementary Data). The synthesized derivatives were characterized by their melting point, TLC R_f value, absorption, and fluorescence maxima.

In the present work, the mass spectra of synthesized amidines were studied. Almost all spectra have a peak of the 1-phenyl-naphthalene (*M* = 201) ion, which is usual for benzanthrone derivatives losing C=O and amidine side chain [23]. Besides, similarly to other N-containing derivatives of benzanthrone [24], the following peaks are observed: a peak of molecular ion of unsubstituted benzanthrone (*M* = 230), a peak of ions [BA-N=C]⁺ (*M* = 256) and [BA-N=CH₂]⁺ (*M* = 258), a peak of molecular ion of 3-aminobenzanthrone (*M* = 245), and a peak of ion [BA-N=CH-CH₂]⁺ (*M* = 270). In addition, the mass spectrum of dyes **2**, **5**, **6** and **7** has a Ph⁺ peak (*M* = 77) in contrast to other derivatives that have no phenyl group.

The thermal stability of dyes is one of the key requirements in some practical applications. In order to gain more insight into these dyes, **5**, **6**, **7** and **8** were subjected to the thermogravimetric analysis to investigate their thermal stabilities. The thermal stability studies were performed at a heating rate of 10 °C/min. Above

330–400 °C, the thermogravimetric curves of these compounds show a major loss in weight, with decomposition temperatures 338, 379, 402, and 367 °C for derivatives **5–8**, respectively. These results confirm that the prepared dyes are thermally stable compounds.

Spectroscopic features

Photophysical properties of dyes **2–8** consisting of donor (amidine) and acceptor (carbonyl) units were investigated in various organic solvents with different dielectric constants. Positions of maxima of the absorption and emission bands of the studied dye solutions are presented in Tables 2 and 3. Absorption and emission spectra of amidines **2–8** was recorded in eight different organic solvents with a wide range of polarities (see absorption and emission spectra for derivative **4** in Fig. 2). Generally speaking, it could be seen that absorption spectra do not show significant variation with solvents.

The electronic absorption spectra of the prepared dyes (Fig. 3) show bands around 210–230 nm, 250–280 nm, and a broad long-wave band around 415–490 nm (log ε = 3.68–4.43), which has a charge transfer character, due to π → π* electron transfer during the S₀ → S₁ transition. The charge transfer in benzanthrone dyes occurs from the electron donor–acceptor interaction between the electron-donating substituents at a C-3 position and an electron-accepting carbonyl group of the chromophoric system [3]. The long-wave absorption maximum of the investigated derivatives in chloroform solution is similar to that of initial 3-aminobenzanthrone (470 nm), the absorption band of the amidines in ethanol solution is hypsochromically shifted by 50–100 nm, if compared to that of amine **1** (518 nm), due to the weaker interaction between the amidine group and the π-electron system of benzanthrone in contrast to interaction between the amino group and the aromatic core. It is interesting that amidines **5** in dimethylsulfoxide solution has two long-absorption bands with the same extinction at 448 and 466 nm.

Emission spectra of the studied dyes were recorded in solution and in solid state upon excitation of the samples at the lowest energy absorption band. The obtained compounds are strongly fluorescent in solutions (except the dyes **3** and **7** in hexane) in the region of 505–540 nm (in hexane) to 560–665 nm (in ethanol) and display large bathochromic shifts (up to 4000 cm⁻¹) from hexane to ethanol solutions with regard to the amino derivatives for which this shift is about 1000 cm⁻¹ [7,8]. In comparison with amine **1** (627 nm), all studied amidines showed a hypsochromic shift of emission maxima in chloroform solutions. But in ethanol solutions, a bathochromic shift (for amidines **2**, **5**) or a hypsochromic shift are observed in comparison with amine **1** (659 nm).

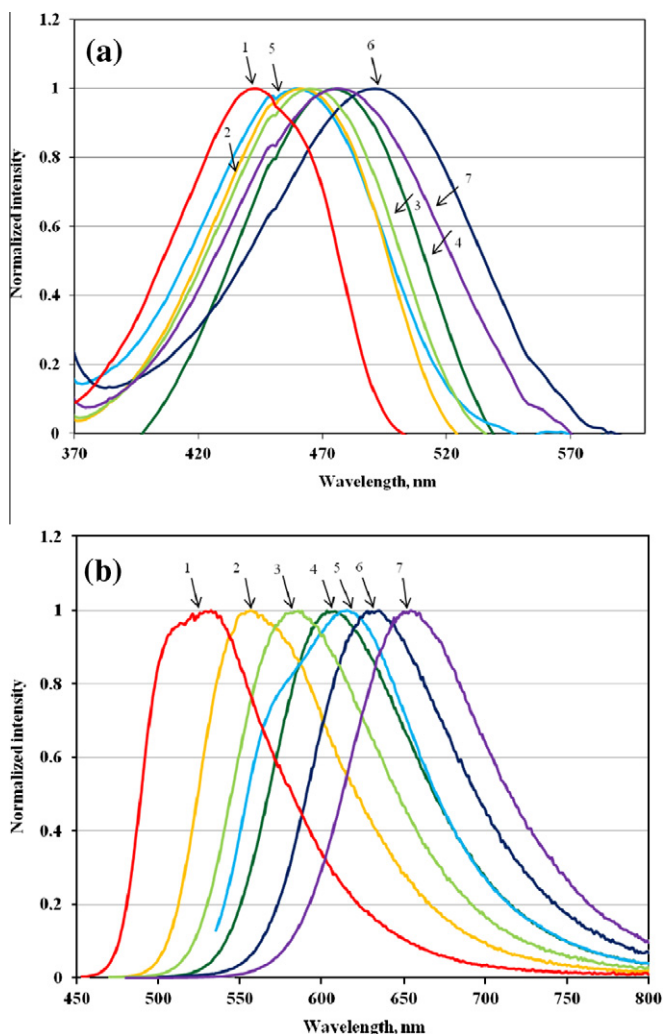
The effect of polarity of the medium on fluorescence is more pronounced than on the absorption spectrum. This is because the intramolecular charge transfer effect leads to a large dipole

Table 2
Absorption maxima of prepared dyes in organic solvents (concentration 10⁻⁵ M).

	Absorption λ _{abs} (log ε) (nm)								
	2	3	4	5	6	7	8	9	10
Hexane	429 (4.16)	–	443 (4.35)	430 (3.68)	426 (3.69)	434 (4.11)	–	432 (3.96)	427 (4.13)
Benzene	445 (4.21)	418 (4.40)	461 (4.31)	446 (3.90)	444 (4.22)	448 (4.24)	418 (4.40)	447 (3.91)	443 (4.06)
CHCl ₃	448 (4.18)	414 (4.41)	460 (4.25)	448 (3.94)	448 (4.27)	460 (4.26)	414 (4.41)	448 (4.11)	448 (4.09)
EtOAc	448 (4.26)	420 (4.42)	465 (4.30)	448 (3.88)	448 (4.24)	449 (4.26)	420 (4.43)	449 (4.11)	448 (4.13)
Acetone	457 (4.16)	420 (4.43)	474 (4.24)	448 (3.87)	458 (4.22)	461 (4.24)	420 (4.43)	449 (4.06)	447 (3.99)
Ethanol	466 (4.17)	420 (4.40)	476 (4.12)	464 (3.80)	462 (4.15)	465 (4.13)	420 (4.40)	448 (4.07)	448 (3.99)
DMF	464 (4.21)	427 (4.40)	484 (4.31)	465 (3.83)	468 (4.23)	470 (4.19)	427 (4.40)	467 (4.14)	472 (4.06)
DMSO	468 (4.22)	430 (4.41)	491 (4.35)	448 (4.00)	474 (4.21)	475 (4.18)	430 (4.41)	473 (4.13)	472 (4.02)

Table 3
Fluorescence maxima of prepared dyes in organic solvents (concentration 10^{-5} M).

	Fluorescence λ_{em} (Φ_0) (nm)									
	2	3	4	5	6	7	8	9	10	
Hexane	527 (0.28)		532 (0.70)	529 (0.67)	536 (0.62)	–	507	525 (0.59)	513 (0.29)	
Benzene	554 (0.37)	508 (0.43)	556 (0.74)	558 (0.81)	544 (0.59)	546 (0.84)	549 (0.79)	565 (0.63)	543 (0.32)	
CHCl ₃	603 (0.29)	527 (0.39)	615 (0.72)	603 (0.73)	580 (0.58)	577 (0.78)	546 (0.78)	608 (0.52)	585 (0.28)	
EtOAc	584 (0.30)	513 (0.37)	586 (0.72)	585 (0.59)	571 (0.57)	569 (0.77)	551 (0.75)	596 (0.51)	569 (0.23)	
Acetone	605 (0.18)	542 (0.28)	603 (0.65)	608 (0.54)	590 (0.45)	593 (0.79)	543 (0.68)	644 (0.46)	590 (0.18)	
Ethanol	663 (0.16)	560 (0.33)	655 (0.70)	662 (0.56)	644 (0.29)	641 (0.83)	573 (0.63)	665 (0.15)	643 (0.08)	
DMF	624 (0.15)	532 (0.29)	615 (0.41)	628 (0.47)	605 (0.23)	603 (0.53)	535 (0.49)	636 (0.12)	614 (0.09)	
DMSO	634 (0.16)	544 (0.22)	635 (0.28)	652 (0.23)	620 (0.21)	633 (0.31)	572 (0.37)	644 (0.14)	624 (0.11)	

**Fig. 2.** The UV-vis (a) and fluorescence emission (b) spectra of amidine **4** (1×10^{-5} mol l⁻¹) in hexane (1), benzene (2), ethyl acetate (3), acetone (4), chloroform (5), DMSO (6) and ethanol (7), respectively.

moment in the excited state. Therefore the studied dyes are more polar in the excited than ground state. The different behavior in absorption and emission is related to the magnitude of the solvent effect on the energy of states during electronic transition. There, it can be observed that the lack of effect on the absorption solvatochromism might be due to the fact that both states, ground and excited, are not equally stabilized by the different solvents under study (and so no significant variations occur in the energy of both states) or, on the other hand, the same degree of stabilization could occur for both. Therefore, for these two possibilities, the energy of

transition is almost the same and, consequently, a net change is not observed in the absorption spectra recorded in each case. As seen from Table 4, the Stokes shift was bigger in the case of more polar solvents, indicating the intramolecular charge transfer character of the excited state.

The solvatochromic effect in emission is clearly observed under a UV lamp irradiation, as it is depicted in Fig. 4, where solutions of dye **4** in *n*-hexane, benzene, chloroform, acetone, and dimethylsulfoxide are shown. A net red shift can be observed in Fig. 4 showing the change from *n*-hexane through to dimethylsulfoxide in accordance with the increasing polarity of the solvents.

As seen from Table 2, with an increase of solvent polarity, the fluorescence quantum yields of the studied dyes decreased with a remarkable red shift. In a polar solvent with a relatively high hydrophilicity, the conformation of the dye molecule is probably twisted, and the twisted intramolecular charge transfer state (TICT) emerges, which red shifts and weakens the emission of fluorophore [1,25]. Therefore, the red shift and weakening of intensity with growing solvent polarity might be caused by TICT processes.

Interesting results were received from photophysical properties of the prepared dyes in the solid state. Crystals of amidines **2**, **3**, **4**, **5** and **10** were obtained by recrystallization from benzene solutions. Compounds **7** and **8**, however, were precipitated in an amorphous state after recrystallization from various solutions (chloroform, benzene, ethanol, and acetone solutions). Amidine **9** forms crystals as solvate with benzene, but these transform into amorphous powder after quickly losing molecules of the solvent. Interestingly, derivatives **3** and **10** also form solvate but with water molecules, catching it during precipitation from the reacting mixture. It was found that dyes **3** and **4** do not emit in crystals, but have a weak luminescence in amorphous powder. Compounds **2**, **5**, **6**, **7**, **9** and **10** exhibit a solid-state luminescence in both crystalline and amorphous states. Dyes **5** and **9** are characterized by an especially high solid-state luminescence (see Fig. 5). Amidines **2**, **5**, **6**, **7**, **9** and **10** exhibit a bright yellow–orange or red luminescence upon excitation at both 254 and 365 nm. Maxima of solid-state luminescence of dyes **2**, **5**, **6**, **7**, **9** and **10** are observed at 602, 632, 589, 645, 614, and 653 nm, respectively.

To elucidate the effect of crystal packing on solid-state luminescence properties, we performed an X-ray crystallographic analysis.

Crystal structure analysis

The structures of **2–5** and **10** were established by the X-ray diffraction. The main crystallographic data and refinement parameters of the crystal structures are listed in Table 5.

The molecular structures of the investigated compounds and atomic thermal ellipsoid are shown in Fig. 6. The molecular structure of **2** is characterized by two plane fragments: one of them is a benzantrone system and the second is a phenylacetamide fragment. The dihedral angle between the planes of these fragments is equal to 63.8°. In the crystal structure, there are intermolecular

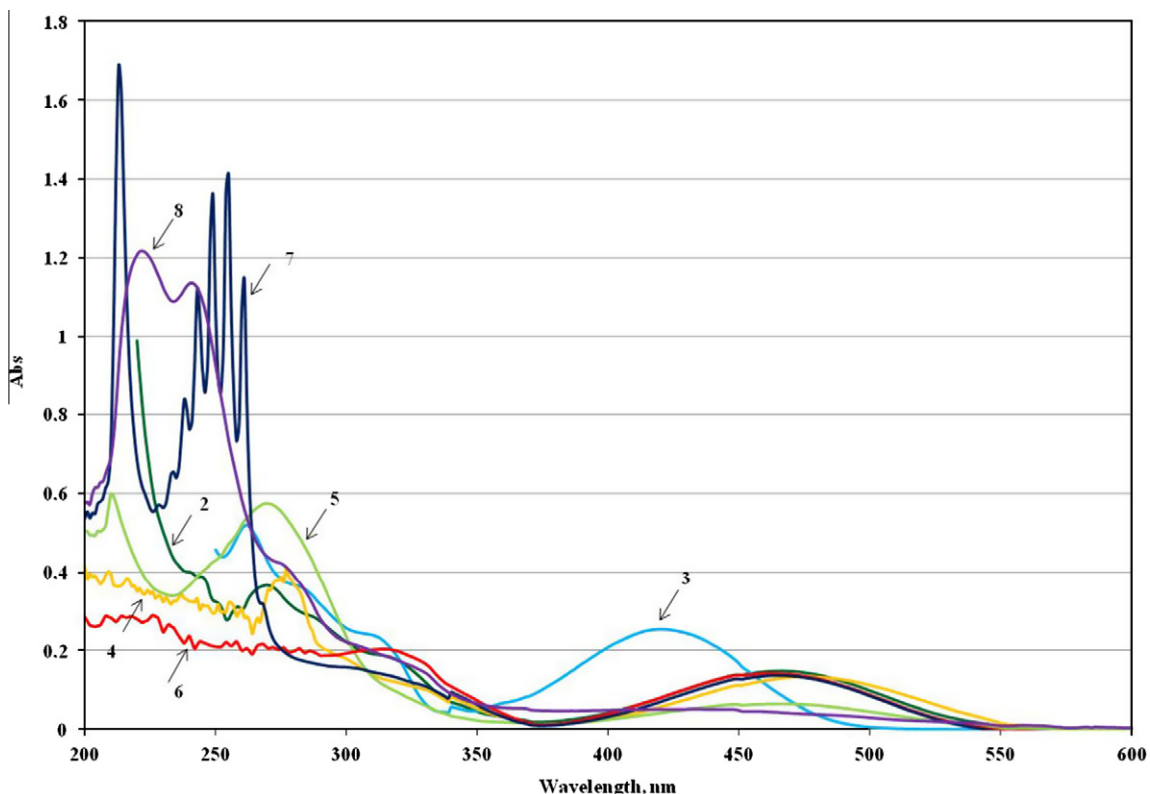


Fig. 3. Absorption spectra of amidines 2–8 in ethanol solution.

Table 4
Stokes shift of prepared dyes in organic solvents (concentration 10^{-5} M).

	Stock shift (cm^{-1})								
	2	3	4	5	6	7	8	9	10
Hexane	4335		3776	4352	4817		–	4100	3926
Benzene	4421	4238	3706	4501	4141	4006	5708	4672	4157
CHCl_3	5737	5180	5479	5737	5080	4408	5840	5874	5227
EtOAc	5198	4317	4440	5227	4808	4697	5661	5493	4746
Acetone	5353	5360	4513	5874	4885	4829	5394	6744	5422
Ethanol	6376	5953	5741	6446	6117	5904	6358	7283	6769
DMF	5526	4622	4401	5581	4839	4693	4727	5690	4899
DMSO	5595	4874	4619	6984	4968	5255	5773	5614	5160

hydrogen bonds of $\text{NH}\cdots\text{O}$ type with length $2.910(3)$ Å ($\text{H}\cdots\text{O} = 1.89$ Å, $\text{N}-\text{H}\cdots\text{O} = 167^\circ$). The chains along crystallographic axis a are formed in the crystal structure by means of these H-bonds. The graph set of these chains is C (10) in accordance with the classification of hydrogen-bond motifs in crystals [31]. There are also π – π stacking interactions in the structure: two benzanthrone systems connected by the center of inversion partially overlap; the distance between parallel benzanthrone planes is 3.414 Å.

In accordance with X-ray analysis data of **3** hydrate, there are two independent molecules in the asymmetric unit. Two molecules of **3** and two water molecules bond by means of $\text{OH}\cdots\text{O}$ and $\text{NH}\cdots\text{O}$ types intermolecular hydrogen bonds and form pseudocentrosymmetrical rings with the graph set $R_4^2(24)$ in accordance with [31]. The lengths of the $\text{OH}\cdots\text{O}$ type hydrogen bonds



Fig. 4. Fluorescence solvatochromism of dye **4** in organic solvents. From left to right: n -hexane, benzene, chloroform, acetone and dimethylsulfoxide.

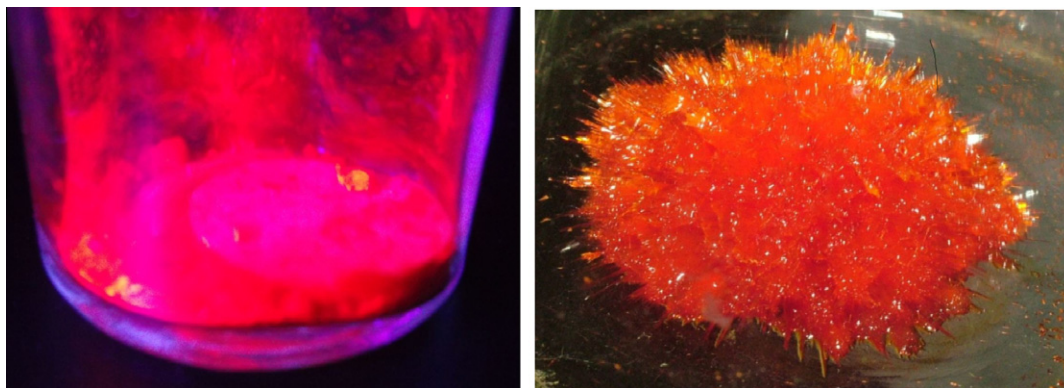


Fig. 5. Solid-state fluorescence of dyes **5** and **9** upon UV excitation at 365 nm.

Table 5
Crystal data for the studied compounds.

	2	3	4	5	10
Brutto-formula	C ₂₅ H ₁₈ N ₂ O	C ₁₉ H ₁₄ N ₂ O·H ₂ O	C ₂₂ H ₂₀ N ₂ O	C ₂₆ H ₂₀ N ₂ O	C ₂₀ H ₁₆ N ₂ O·H ₂ O
Formula weight	362.43	304.34	328.42	376.46	318.36
Crystal system	Monoclinic	Orthorhombic	Monoclinic	Monoclinic	Monoclinic
<i>a</i> (Å)	6.8530(5)	8.6174(2)	8.1933(3)	13.1472(4)	13.1890(5)
<i>b</i> (Å)	22.691(2)	13.6136(3)	17.5476(6)	7.2323(2)	8.6849(4)
<i>c</i> (Å)	11.7584(9)	25.5817(6)	11.7909(5)	20.0270(5)	13.5801(5)
β (°)	98.117(4)	90.0	96.874(1)	90.628(2)	93.920(3)
<i>V</i> (Å ³)	1810.1(2)	3001.1(1)	1683.0(1)	1904.14(9)	1551.9(1)
Space group	<i>P</i> 2 ₁ / <i>c</i>	<i>P</i> <i>bc</i> 2 ₁	<i>P</i> 2 ₁ / <i>n</i>	<i>P</i> 2 ₁ / <i>n</i>	<i>P</i> 2 ₁ / <i>c</i>
<i>Z</i>	4	8	4	4	4
μ (mm ⁻¹)	0.082	0.089	0.080	0.080	0.089
Density (calc.) (g/cm ³)	1.330	1.347	1.296	1.313	1.363
2 θ _{max} for data (°)	57.0	60.0	60.0	60.0	54.0
Reflection collected	6579	8053	7699	8222	6244
Independent reflections	4551 (<i>R</i> _{int} = 0.046)	4437 (<i>R</i> _{int} = 0.047)	4767 (<i>R</i> _{int} = 0.034)	5349 (<i>R</i> _{int} = 0.034)	3670 (<i>R</i> _{int} = 0.069)
Reflections with <i>I</i> > <i>n</i> σ (<i>I</i>)	2383 (<i>n</i> = 3)	3066 (<i>n</i> = 2)	2951 (<i>n</i> = 3)	3118 (<i>n</i> = 3)	2194 (<i>n</i> = 2)
Final <i>R</i> -factor	0.064	0.057	0.061	0.047	0.096
<i>wR</i> ₂ index for all data	0.231	0.169	0.232	0.282	0.347
Temperature (°C)	-100	-100	-100	-100	-80
Using programs	SIR97 [26], maXus [27]	SHELXS97 [28], SHELXL97 [28]	SIR92 [29], maXus [27]	DETMEX [30], maXus [27]	SHELXS97 [28], SHELXL97 [28]
CCDC deposition number	CCDC 884478	CCDC 884884	CCDC 884480	CCDC 884481	CCDC 884482

are 2.918(4) and 2.921(4) Å; these values for the NH \cdots O bonds are 2.961(4) and 2.962(4) Å. Furthermore, OH \cdots N type intermolecular H-bonds are found. The lengths of these hydrogen bonds are 2.875(4) and 2.897(4) Å. These bonds form new motifs in the crystal structure, namely chains of C(6). The H-bonds in this structure create the molecular layers which are parallel to the crystallographic plane (001). Fig. 7 illustrates a view of the layer along the crystallographic axis *c*. There are weak stacking interactions between benzanthrone systems of molecules, with distances corresponding to the sum of van der Waals radii.

An intermolecular contact between amidine carbon and carbonyl oxygen (3.241(3) Å) should be noted in crystal structures of **4**; this contact can be considered as a weak CH \cdots O type hydrogen bond (H \cdots O = 2.57 Å, N–H \cdots O = 124°). The stacking interaction is practically absent (the distance between parallel benzanthrone systems in the crystal is equal to 3.728 Å).

Fig. 8 shows projections of crystal structure **5** along the monoclinic axis. Similar to structure **2**, there are intermolecular H-bonds of the NH \cdots O type (N \cdots O = 2.955(2) Å, H \cdots O = 2.05 Å, N–H \cdots O = 174°) with the graph set C(10). In the crystal structure by means of these H-bonds the chains are formed along crystallographic direction $[\bar{1}01]$. The crystal structure is characterized by strong π – π stacking interactions: benzanthrone systems lie parallel to the crystallographic plane (121), and the distance between the planes is 3.348 Å (the shortest contact between two carbons is 3.351 Å). The perspective view of the stack of molecules **5** is

shown in Fig. 9. These peculiarities of crystal structure **5** perhaps are grounds of/might make the basis for luminescent properties of **5**.

Dye **10** is a hydrate compound; there is an intermolecular H-bond system between water molecules and **10**, which is similar to **3**. There are also weak stacking interactions between benzanthrone systems of **10**.

It is known that strong intermolecular π – π interactions and/or continuous intermolecular hydrogen bonding between neighboring molecules is a principal factor of luminescence quenching in the solid state [32]. But according to our data, most efficient luminescence is observed in the dye characterized by a stronger π – π stacking interactions, dye **5** in our case. Such packing of crystal **5** likely promotes the exciton–phonon interactions which are intensified by shortened contacts in the crystal structure. Effective luminescence in solid state is also attributed to restricted intramolecular motions [1]. A more detailed study with a larger number of samples is needed for better understanding the correlations between solid-state luminescence and molecular packing structure of benzanthrone dyes.

Quantum chemical calculations

To better understand the nature of electronic spectra of benzanthrone **2**–**10**, the quantum chemical calculations were carried out. For each compound, the geometry optimization for two possible

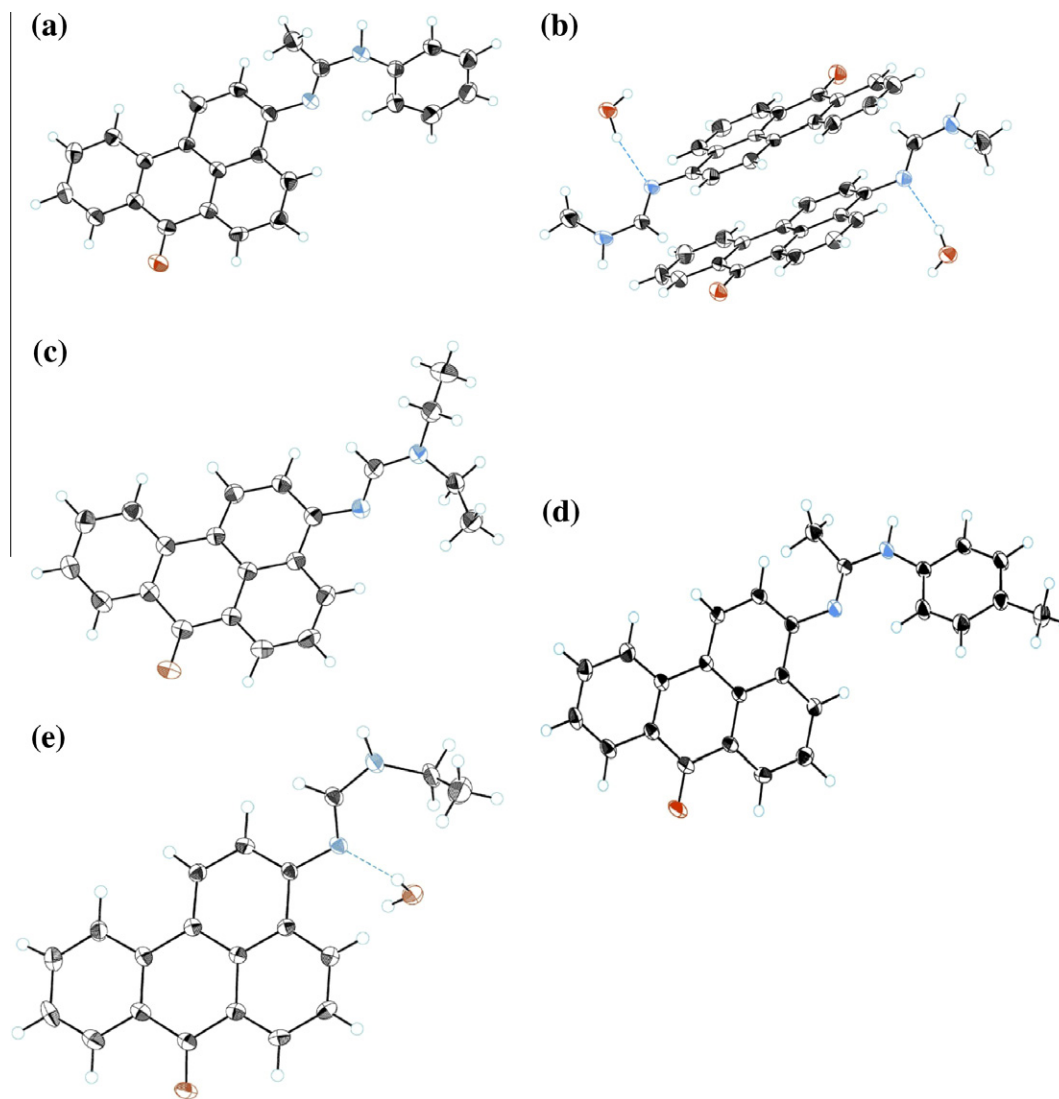


Fig. 6. ORTEP diagrams of the X-ray structure of **2** (a), **3** (b), **4** (c), **5** (d) and **10** (e).

isomers was performed by the AM1 method. As the calculated electronic energies of isomers A and B (Fig. 10) do not show a big difference, and rotation barrier of the amidine group is also low, the preferred structures are those with a different orientation of the amidine group in each case (crystallographic data, though, prove that structures of type A have priority).

The *ab initio* calculations using DFT give the same geometries (the differences are insignificant) and almost the same distribution of charges (differences are also small), but HOMO energies calculated with this method (~ -5.2 eV) look too high. It is obvious that the first ionization potential must be greater (about $(-)$ 7–8 eV) for this class of compounds.

The substituents R, R₁ and R₂ do not show a great influence on HOMO and LUMO energies calculated by any of the used method, although their influence on HOMO is more remarkable than on LUMO. An insignificant influence of substituents R, R₁ and R₂ on charges of the nearest carbon atoms is noticed in benzanthrone system. The substituents mainly have an effect on the carbon atom of amidine group, where charges vary from ~ 0.08 to 0.19 e. On the other hand, the substituents in the amidine fragment affect notably on the molecules dipole moments. The dipole moments vary, depending on substituents, from 3.9 D to 7.7 D (AM1 method) or

from 6.0D to 10.4D (ZINDO/S method) (Table 6). The dipole moments grow if the molecules in the amidine fragment have electron-donating groups (Me, Et). Also, molecules with the structure of type A show greater dipole moments than structures of type B (structures **5** and **8**, where amidine substituent is less or more shifted out from the benzanthrone plane, make an exception).

The electronic spectra of benzanthrone were calculated using the ZINDO/S method. Calculations show an intensive (oscillator strength is about 0.6–0.9), long-wave absorption band at 370–380 nm. This absorption is generally an electron shift from HOMO to LUMO. Both orbitals are mainly localized in the benzanthrone fragment (Fig. 11), whereas the amidine group investment in this shift is small.

Long-wave absorption causes a notable increase of the system dipole moment by about 3–4 D (Table 6). So, the excited state dipole moments reach 10–14.7 D. As the molecules are strongly polar compounds, it is not surprising that in real spectra, the long-wave absorption band is shifted by about 60–70 nm due to solvation effect (Table 2). This shift is caused by intermolecular interactions or interactions of molecules with the solvent, and it confirms the large solvatochromic effect. The next notable absorption band for amidines **2–10** is at about 280–300 nm. These bands

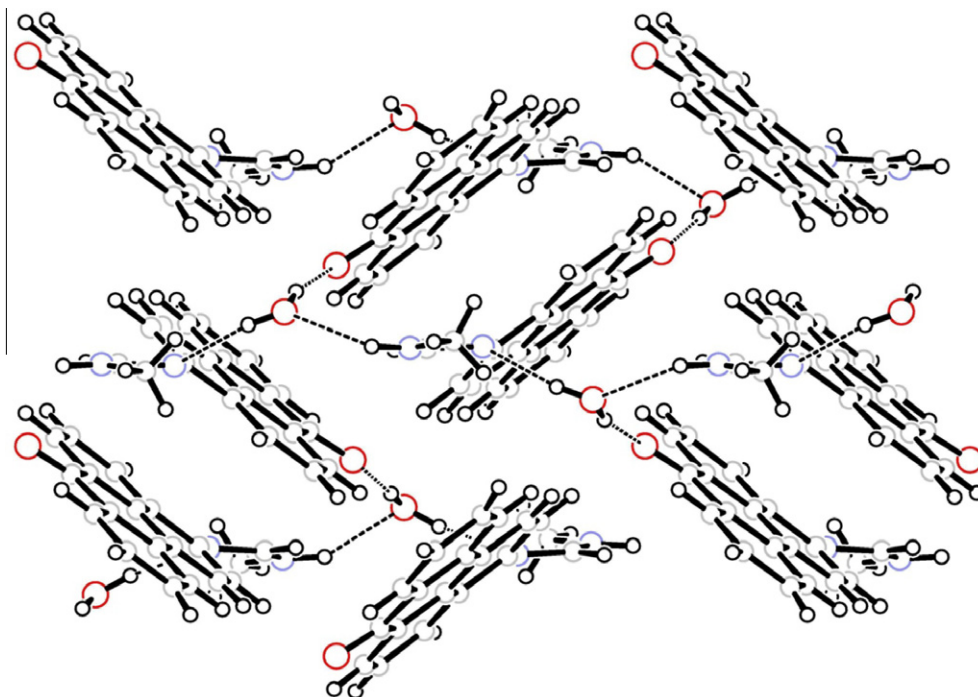


Fig. 7. A molecular layer in the crystal structure of dye 3.

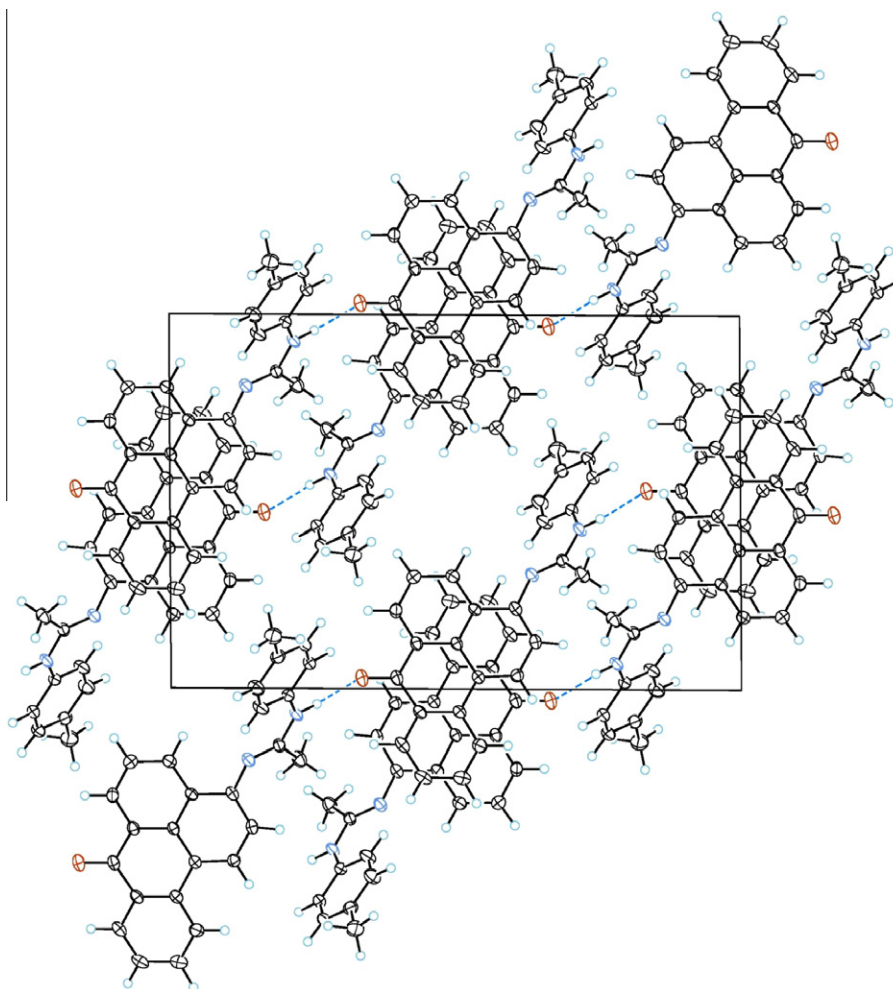


Fig. 8. Projection of the crystal structure of dye 5 on crystallographic plane (010).

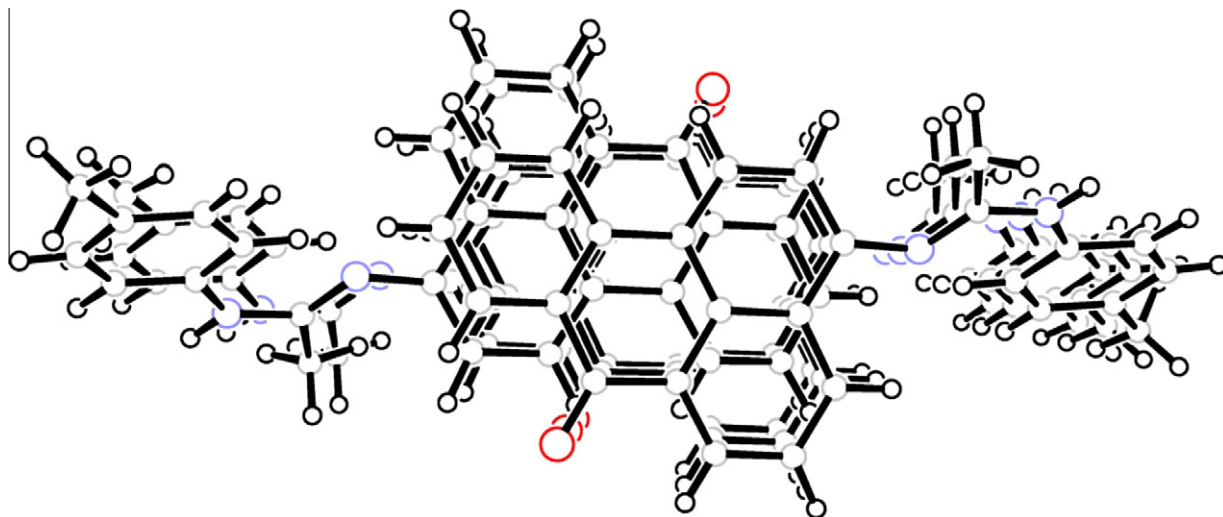


Fig. 9. A stack of molecules in the crystal structure of dye 5.

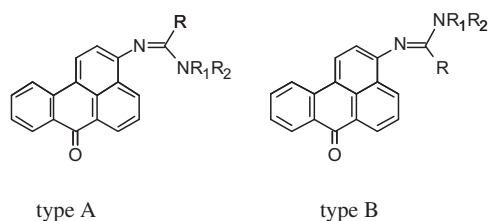


Fig. 10. Possible benzanthrone amidine isomers.

are characterized by a not so strong absorption (oscillator strength is about 0.1), and these mostly consist of the electron shift between different orbitals.

Conclusion

Synthesis and spectral properties of novel benzanthrone N-substituted amidine dyes were described. Novel dyes were synthesized in good yields (52–92%) via the condensation reaction of 3-aminobenzanthrone with corresponding amides. Compounds

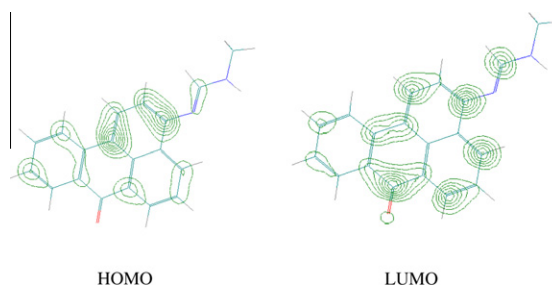


Fig. 11. HOMO and LUMO localization for amidine 3A (ZINDO/S).

were characterized by NMR, FT-IR, UV-vis and X-ray crystallography. The results of thermogravimetric analysis showed that these dyes were thermally stable and therefore may have various applications. The synthesized dyes absorb at 410–490 nm with high extinction coefficients, have relatively large Stokes' shifts (up to 4800 cm^{-1} in hexane and 7300 cm^{-1} in ethanol), and emit at 505–665 nm. Some of the prepared dyes exhibit strong luminescence in solid state. The relationships between the solid-state

Table 6
Quantum chemical calculations of benzanthrone amidines 2–10.

Structure	AM1		ZINDO/S		<i>ab initio</i> B3LYP/6-31G(d)		λ_{max} (nm) (oscillator strength)	μ_{ground} (D)	μ_{excited} (D)
	HOMO (eV)	LUMO (eV)	HOMO (eV)	LUMO (eV)	HOMO (eV)	LUMO (eV)			
2A	-8.24	-1.18	-7.22	-0.93	-5.37	-2.08	371.8 (0.7062)	9.3	13.6
2B	-8.37	-1.27	-7.29	-0.95	-5.29	-2.10	368.1 (0.6058)	6.1	9.9
3A	-8.03	-1.16	-7.18	-1.00	-5.22	-1.98	382.6 (0.8733)	10.0	14.0
3B	-8.29	-1.23	-7.30	-0.97	-5.28	-1.99	372.5 (0.6259)	6.2	10.0
4A	-8.19	-1.17	-7.25	-0.94	-5.13	-1.96	374.9 (0.6199)	8.1	12.5
4B	-8.23	-1.13	-7.25	-0.94	-5.20	-1.98	374.4 (0.6709)	7.6	11.7
5A	-8.26	-1.20	-7.26	-0.94	-5.25	-2.07	369.7 (0.6238)	7.0	10.8
5B	-8.33	-1.23	-7.27	-0.93	-5.22	-1.98	370.5 (0.7168)	8.1	12.2
6A	-8.40	-1.29	-7.35	-1.00	-5.34	-2.10	370.6 (0.7254)	6.8	10.6
6B	-8.28	-1.27	-7.31	-0.99	-5.40	-2.16	368.1 (0.6444)	6.0	9.9
7A	-8.14	-1.17	-7.22	-0.97	-5.17	-1.96	374.1 (0.8148)	9.3	13.3
7B	-8.27	-1.22	-7.28	-0.96	-5.27	-2.04	368.2 (0.6645)	6.5	10.2
8A	-8.03	-1.27	-7.22	-1.11	-5.29	-2.01	388.0 (0.8173)	6.6	10.4
8B	-8.20	-1.20	-7.30	-1.02	-5.32	-2.04	374.6 (0.7786)	8.8	12.7
9A	-7.95	-1.12	-7.12	-0.95	-5.16	-1.95	383.7 (0.8988)	10.4	14.7
9B	-7.86	-1.21	-7.07	-1.03	-5.16	-1.94	394.8 (0.8989)	7.6	11.8
10A	-8.00	-1.13	-7.17	-0.99	-5.20	-1.97	382.9 (0.8720)	10.1	14.1
10B	-8.26	-1.20	-7.29	-0.96	-5.19	-1.96	372.7 (0.6233)	6.4	10.1

photophysical properties and chemical and crystal structures of the synthesized dyes are discussed. These aimed dyes are sensitive to the solvent polarity, showing positive solvatochromism and reduced fluorescence in polar solvents. These characteristics of the prepared benzanthrone dyes demonstrate their potential as biomedical probes for proteins, lipids, and cells. Such dyes can be also utilized as suitable sensing probes for checking solvent polarity.

Acknowledgement

This work was supported by the grant from European Social Fund (Project Number 2009/0205/1DP/1.1.1.2.0/09/APIA/VIAA/152).

Appendix A. Supplementary material

Supplementary data associated with this article can be found, in the online version, at <http://dx.doi.org/10.1016/j.saa.2012.09.104>.

References

- [1] B. Valeur, *Molecular Fluorescence: Principles and Applications*, Wiley-VCH, Weinheim, 2001.
- [2] B.M. Krasovitskii, B.M. Bolotin, *Organic Luminescent Materials*, VCH Publishers, 1988.
- [3] O.R. Hrolova, N.I. Kunavin, I.V. Komlev, M.A. Tavrizova, *J. Appl. Spectrosc.* 41 (1984) 53–58.
- [4] F. Carlini, C. Paffoni, G. Boffa, *Dyes Pigm.* 3 (1982) 59–69.
- [5] J. Slavik, *Fluorescent Probes in Cell Biology*, CRC Press, Boca Raton, Ann Arbor; London, Tokyo, 1994.
- [6] G.E. Dobretsov, *Fluorescent Probes for Studying Cells, Membranes and Proteins*, Nauka, Moscow, 1989.
- [7] E. M. Kirilova, I. Meirovics, S.V. Belyakov, *Chem. Heterocycl. Comp.* 7 (2002) 896–900.
- [8] E.M. Kirilova, I. Kalnina, G.K. Kirilov, I. Meirovics, *J. Fluoresc.* 18 (2008) 645–648.
- [9] E.M. Kirilova, S.V. Belyakov, I. Kalnina, in: G. Vayssilov, R. Nikolova (Eds.), *Topics in Chemistry & Materials Science*, vol. 3, Heron Press, Sofia, 2009, pp. 19–28.
- [10] V.M. Trusova, E. Kirilova, I. Kalnina, G. Kirilov, O.A. Zhytniakivska, P.V. Fedorov, G. Gorbenko, *J. Fluoresc.* 22 (2012) 953–959.
- [11] J. Barker, M. Kilner, *Coord. Chem. Rev.* 133 (1994) 219–300.
- [12] M.V. Kazankov, G.I. Putsa, L.L. Mukhina, *Chem. Heterocycl. Comp.* 9 (1973) 563–569.
- [13] Y. Liu, K. Ye, Y. Fan, et al., *Chem. Commun.* 25 (2009) 3699–3701.
- [14] M.J.S. Dewar, E.G. Zoebisch, E.F. Healy, J.J.P. Stewart, *J. Am. Chem. Soc.* 107 (1985) 3902–3909.
- [15] J.J.P. Stewart, *J. Comput. – Aid. Mol. Des.* 4 (1990) 1–105.
- [16] J. Ridley, M. Zerner, *Theor. Chim. Acta* 32 (1973) 111.
- [17] J.E. Ridley, M.C. Zerner, *Theor. Chim. Acta* 42 (1976) 223.
- [18] M.C. Zerner, G.H. Loew, R.F. Kirchner, U.T. Mueler-Westerhoff, *J. Am. Chem. Soc.* 102 (1980) 589.
- [19] R.G. Parr, W. Yan, *Density-functional Theory of Atoms and Molecules*, Oxford University Press, Oxford, England, 1989.
- [20] A. Luttringhaus, H. Neresheimer, *Justus Liebigs Annalen der Chemie.* 273 (1929) 259–289.
- [21] I. Grabchev, I. Moneva, *Dyes Pigm.* 38 (1998) 155–160.
- [22] H. Brederbeck, R. Gompper, K. Klemm, H. Rempfer, *Chem. Ber.* 92 (1959) 837–849.
- [23] Z. Abliz, T. Ueda, K. Kubogata, S. Iwashima, *Org. Mass Spectrom.* 25 (1990) 345–352.
- [24] M. Holcapek, K. Volna, D. Vanerkova, *Dyes Pigm.* 75 (2007) 156–165.
- [25] Z.R. Grabowski, K. Rotkiewicz, *Chem. Rev.* 103 (2003) 3899–4031.
- [26] A. Altomare, M. Burla, M. Camalli, G. Cascarano, C. Giacovazzo, A. Guagliardi, A. Moliterni, R. Spagna, *J. Appl. Crystallogr.* 32 (1999) 115–119.
- [27] S. Mackay, W. Dong, C. Edwards, A. Henderson, C.J. Gilmore, N. Stewart, K. Shankland, A. Donald, *maxUS, Integrated Crystallography Software*, Bruker-Nonius and University of Glasgow, 2003.
- [28] G.M. Sheldrick, *Acta Crystallogr. A* 64 (2008) 112–122.
- [29] A. Altomare, G. Cascarano, C. Giacovazzo, A. Guagliardi, M.C. Burla, G. Polidori, M. Camalli, *J. Appl. Crystallogr.* 27 (1994) 435–436.
- [30] A.F. Mishnev, S.V. Belyakov, *Krystallografiya* 33 (1988) 835–837.
- [31] M.C. Etter, *Acc. Chem. Res.* 23 (1990) 120–126.
- [32] H. Langhals, T. Potrawa, H. Nöth, G. Linti, *Angew. Chem.* 101 (1989) 497–499.